Please cite this articla as, "T. Tafsirojjaman, S. Fawzia, D. Thambiratnam, Investigation on the behaviour of CFRP strengthened CHS members under Monotonic loading through finite element modelling, Structures. 28 (2020), pp. 297-308 (doi.org/10.1016/j.istruc.2020.08.059)

Investigation on the behaviour of CFRP strengthened CHS members under Monotonic loading through finite element modelling

T. Tafsirojjaman [a], Sabrina Fawzia [a, *], David Thambiratnam [a]

[a] School of Civil and Environmental Engineering, Faculty of Science and Engineering, Queensland University of Technology, 2 George Street, Brisbane, QLD 4000, Australia.

([*]Corresponding author: sabrina.fawzia@qut.edu.au, Tel: 61731381012, Fax: 61 7 31381170

Email addresses: tafsirojjaman@hdr.qut.edu.au (T. Tafsirojjaman), sabrina.fawzia@qut.edu.au (Sabrina Fawzia), d.thambiratnam@qut.edu.au (David Thambiratnam)

Abstract

During the past several years, civil infrastructure has made extensive use of tubular hollow steel members as structural elements. However, the rehabilitation and strengthening of tubular hollow steel members is a major concern due to design errors, environmental effects, reduction in material properties over time caused by corrosion and the need to withstand increased loads. A comprehensive investigation on the strengthening of tubular hollow steel members is therefore required. Although carbon fibre reinforced polymer (CFRP) strengthening technique has shown its effectiveness to improve the structural response of different steel members, studies on the structural response of circular hollow section (CHS) steel members strengthened with CFRP is limited. In the present study, an effective finite element (FE) model is first developed by comparing the FE model simulated results with the authors' experimental results. This is followed by a parametric study on the effect of the bond length of CFRP, number of CFRP layers, ratio of CFRP thickness to CHS wall thickness, diameter to thickness ratio of CHS and steel grade of CHS on the structural behaviour of the strengthened member subjected to monotonic loading. These parameters had noteworthy effects on the behaviour of the CFRP strengthened CHS steel members under monotonic loading. The CFRP strengthened CHS steel

members showed an improvement in the moment capacity, secant stiffness, energy dissipation capacity and ductility compared to their bare CHS steel members. It can be concluded that the effectiveness of the CFRP strengthening technique is enhanced with the increase in the ratio of CFRP thickness to CHS wall thickness and/or increasing the diameter to thickness ratio of CHS. In contrast, the effectiveness of the CFRP strengthening technique is decreasing with the increasing of the steel grade.

Keywords: Circular hollow section (CHS) steel members; CFRP; Strengthening; Monotonic loading; FE modelling.

Nomenclature:

COV	Coefficient of variance
E_a	modulus of elasticity of the adhesive
$\sigma_{\max}$	tensile strength of the adhesive
G_I	interlayer fracture toughness of adhesive in mode I
G_{II}	interlayer fracture toughness of adhesive in mode II
k_{nn}	normalised elastic modulus of adhesive in mode I
$k_{ss}=k_{tt}$	normalised elastic modulus of adhesive in mode II and mode III

1. Introduction

The mechanical and performance-based properties of steel members have increasingly benefitted the civil infrastructure scene, especially where complex designs or heavy loading situations exist. The greatest impact have been associated with tubular hollow members as they perform well in compression, bending, and torsion in all directions and they possess a higher resistance to corrosion due to the absence of sharp edges in comparison to open members such as I-sections, channels, equal and unequal angles [1]. Tubular hollow steel members are mostly

used in open areas and buildings as beams and columns, space frames of roofs or lattice girders. Tubular hollow members are also used for architectural and structural purposes in facades today. They have found use not only in onshore structures but also in offshore structures. More specifically, jacket-type offshore structures are built based on the welding of tubular hollow members [2]. The rehabilitation and strengthening of tubular hollow steel members are a major concern due to the design errors, environmental effects, loss of material properties over time due to corrosion and the need to withstand increased loads. Therefore, researchers have paid a vast amount of attention on the rehabilitation and strengthening of tubular hollow steel members.

The original thought process behind retrofitting and reinforcing steel structure members was to weld additional steel plates, however, this would affect the stress distribution as a by-product of the heat produced during the welding process in conjunction with the additional weight of the reinforcement plates. In addition, the welding process would also be susceptible to corrosion and ultimately result in fatigue damage [2]. On the other hand, reinforcement and retrofitting methods with the use of carbon fibre reinforced polymer (CFRP) composites can overcome these disadvantages as there is no welding, heat, or notable extra weight. Other advantages could include a superior strength-weight ratio which is a result of the high tensile strength [3] and resistance to corrosion [4]. The retrofitting option is also incredibly cost-effective as it requires less labour and preparation than welding support plates, easily applicable even with limited access and highly flexibility as it can be shaped to any required form [5,6]. Past research has demonstrated the effectiveness of CFRP strengthening to enhance the impact resistance [7] of steel structures and to reduce their tip displacement under seismic loading [8,9]. Additionally, local buckling was delayed [10,11] and CFRP strengthened CHS steel members showed higher ultimate strength under pure four-point bending [12,13]. Past research also concluded through a four-point bending investigation that FRP strengthening technique

enhanced the durability of steel members in marine environment [14] and in cold weather as well [15].

In all the past research four-point bending tests were used to investigate the bending behaviour of CHS [12–15]. There is however very limited study on the response of a cantilevered CHS member under monotonic loading where the monotonic load applied at the member tip which is allowed to bend and failure occurs at the fixed end and better to investigate the bending behaviour [16]. The authors have experimentally investigated the behaviour of cantilevered CFRP strengthened CHS members under monotonic loading with limited parameters due to the limitations in the experimental process [16]. The present paper aims to enhance this investigation through a numerical approach. Towards this end, a finite element (FE) model was developed in ABAQUS CAE [17] FE software to study the behaviour of the cantilevered CFRP strengthened CHS members under monotonic loading. The accuracy of the developed FE modelling technique was confirmed by comparing the FE model simulated results with the experimental results [16]. Furthermore, a parametric study is conducted to study the effects of the CFRP bond length, number of layers of CFRP, ratio of the CFRP thickness (t_{CFRP}) to CHS wall thickness (t_{CHS}), diameter to thickness ratio of CHS and steel grade on the structural behaviour of the strengthened member subjected to monotonic loading. Results showed that the CFRP strengthened CHS steel members showed an improvement in the moment capacity, secant stiffness, energy dissipation capacity and ductility compared to their bare counterparts. The research gap in the experimental research on the structural response of CFRP strengthened CHS has been covered in the present study. Moreover, the structural behaviour of various CHS members strengthened with CFRP under monotonic loading can be predicted far more cost effectively with the proposed FE model and completed significantly faster than the experimental investigation. Moreover, outcomes of the present study can be used to repair, restore or improve the structural performance of CHS steel members with CFRP.

2. Experimental study

The bending behaviour of bare and CFRP strengthened CHS steel member under monotonic loading has been previously investigated experimentally by the Authors with limited parameters due to the limitations in the experimental process [16]. Identical specimens of steel CHS members (with 4 mm wall thickness, 101.6 mm diameter and 1100 mm length) were used in the experiment. One specimen remained bare and was considered as control specimen, while the other two specimens were strengthened by CFRP with fibre orientation of LHL (three CFRP layers were applied with longitudinal, hoop and longitudinal fibre orientation respectively) with a bond length of 900 mm. There were two types of adhesives named Mbrace saturant and Araldite K630 each of which was as in the strengthening of SB-M-1 and SB-M-2 respectively. One end of the CHS member was fixed while the monotonic load was applied laterally at the free end of the member. The detailed procedure on the preparation of specimens and the process of the experiment can be found in Tafsirojjaman et al. [16].

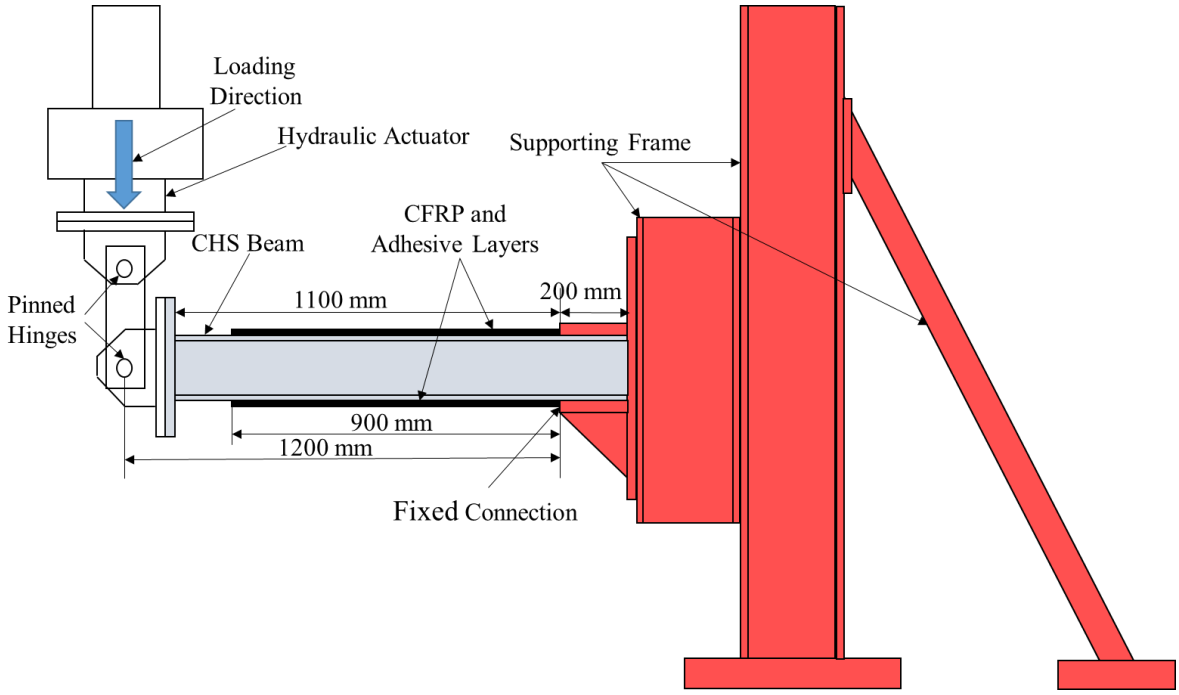

Figure 1: Schematic diagram of the experimental process [16].

Table 1: Specimens details

Specimen notation	Adhesive types	Types of Specimen
BB-M	-	Bare Beam
SB-M-1	Mbrace saturant	Strengthened Beam
SB-M-2	Araldite K630	Strengthened Beam

3. FE modelling and validation

The three-dimensional ABAQUS CAE [17] FE software was used to perform the numerical investigation. Results from the experimental study by the authors were used to validate the developed FE model and numerical simulation by comparing results. Detailed numerical analysis was conducted using the high-performance computer (HPC) at Queensland University of Technology (QUT) to reduce the time taken for simulations.

3.1.1 FE model and element types

3D finite element models of both the bare and CFRP strengthened CHS steel specimens were created using the same parameters of outer diameter of 101.6 mm, wall thickness of 4 mm, length of 1100 mm and bond lengths of 900mm for both the adhesive and CFRP, all as used in the test specimens. The CFRP layer thickness of 0.60 mm was adopted from the experimental measurement of CFRP layer thickness [16]. The adhesive layer thickness of 0.1 mm was assumed based of previous research [18]. A single adhesive bond layer between the steel outer surface and the first CFRP layer was modelled in the FE model as the CFRP layers were applied within wet condition of previous layer and no debonding was noticed between the CFRP layers. An independent reference node located in the cross-sectional centre was created in the supporting end and loading point. All peripheral end nodes were constrained using Multiple Point Constraints (MPC) to that central reference node. The supported end independent reference node enabled to fix all the rotational and translational degrees of freedom while the reference node at the loading point remained free to represent the test setup.

Modelling the steel was undertaken using a 4-node shell elements (S4R) with hourglass control and reduced integration. A three-dimensional 8 node cohesive element (COH3D8) was used for modelling the adhesive layer as it has the capabilities to predict the behaviour and failure of the adhesive [18–20]. Quadrilateral 8-node in-plane continuum shell elements (SC8R) with hourglass control and reduced integration were used to model the CFRP layers as they are capable of accurately predicting the composite failure [18–20]. Solid offsetting orphan mesh with sharing nodes in the outward stacking direction was used to model the continuum and cohesive elements, and the mesh size of both these elements was identical to that of the steel member to enable the constraints between the two. Optimization of element size was determined through a convergence study to ensure the accuracy of the models. Tie constraints were used to create the bonding of the adhesive and CFRP layers to the steel tube surface in the model.

3.1.2 Material model and properties

Elastic and plastic with isotropic strain hardening material model were used to closely depict the inelastic bending behaviour. Steel properties used in the modelling were taken from the experimental study with the elastic modulus of 190 GPa, yield strength of 320 MPa and ultimate strength of 367 MPa [16]. The Poisson's ratio of steel was taken as 0.3 [21].

Coupled cohesive zone modelling with traction separation law was used to model the layer of adhesive between the steel member and CFRP layer. This cohesive model considers both separations and tractions along the normal direction and shear directions (two parallel) to the interface. Mixed-mode failure (QUADS) [17] is used to define the initiation of damage. Benzeggah-Kenane (BK) mixed-mode law [22] which is based on fracture energy was used in ABAQUS to model the evolution of damage through the energy-based softening approach. The adhesive properties given in Table 2 were used in the modelling and taken from previous experimental [16] and numerical studies [12].

Elastic-lamina material model was used for modelling the CFRP layers and the material failure or damage behaviour was defined by Hashin failure criteria [23,24]. Many researchers used this damage model [12,25] due to its suitability to simulate the damage and failure of brittle-elastic material. The modulus of elasticity (E_{IC}) and tensile strength (T^L) used in the modelling was taken from the experimental study [12,16] and given in Table 2. Furthermore, the facture energy of each failure mode was adopted from [18] and displayed in Table 2. Fracture energy is denoted by G and the subscripts f, m, c and t represent the fibre, matrix, compression and tension respectively. Longitudinal direction compressive strength (C^L) of CFRP is assumed as 20% of tensile strength [18]. The tensile/compressive strengths in the transverse direction and the shear strengths in the longitudinal/transverse direction is assumed at 10 percent of the tensile strength [18]. The CFRP Poisson's ratio was taken as 0.33 [12]. The material properties of the adhesive and CFRP used in the present FE modelling are given in Table 2.

Table 2: Material properties of the adhesive and CFRP for FE modelling

Adhesive			CFRP	
Parameter	Mbrace Saturant	Araldite K630	Parameter	Value
E_a	2.86 GPa	6.5 GPa	E_{1C}	75 GPa
$\sigma_{\max}$	46 MPa	33 MPa	E_{2C}	25 MPa
k_{nn}	2.8×10^{13} N/m^3	6.07×10^{13} N/m^3	T^L	987 MPa
$k_{ss}=k_{tt}$	1.4×10^{13} N/m^3	3.03×10^{13} N/m^3	G_{ft}	91,600 N/m
G_I	1000 N/m	1000 N/m	G_{fc}	79,900 N/m
G_{II}	1250 N/m	1250 N/m	G_{mc}	1100 N/m
			G_{mt}	220 N/m

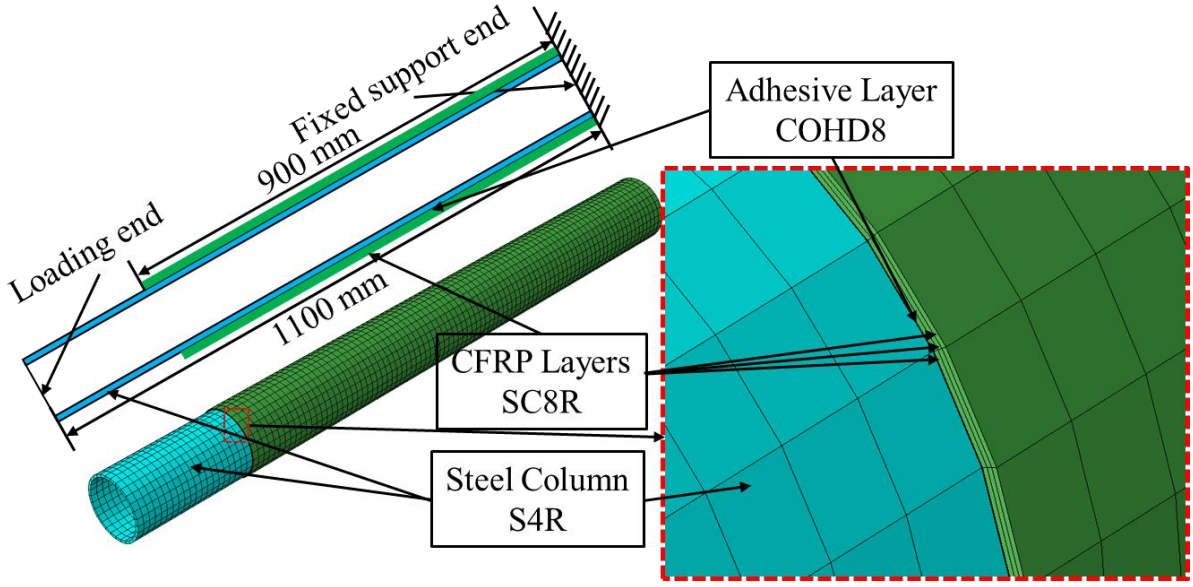

Figure 2: Details of FE model

3.1.3 Validation

The FE modelling technique was validated by comparing the results obtained from the FE model simulation with the experimental results. Figure 3-Figure 5 present the comparisons of the moment capacities of the bare and CFRP strengthened specimens obtained from the FE analysis and experimental tests. The moment capacity responses of the bare and CFRP strengthened CHS steel members obtained from the FE model and the experiments closely match while the ultimate moment capacity COV is 0.021 and the mean ratio is 1.003. Additionally, the comparisons of the experimental and FE simulated secant stiffness and energy dissipation capacity curves for the bare and CFRP strengthened CHS members are given in Figure 6 and Figure 7 respectively. The secant stiffness is calculated by dividing the load by the displacement and energy dissipation capacity is obtained from the enclosed area of the load-displacement curves. The experimental and FE simulated results for the bare and CFRP strengthened CHS members were similar although a small divergence of the FE model simulated results from the experimental results can be noticed at the beginning due to observed uncertain flexibility of sandwiched rigid support connection during monotonic testing [16].

The agreement of experimental and FE results from this discussion confirmed the validation of the presently used FE modelling techniques.

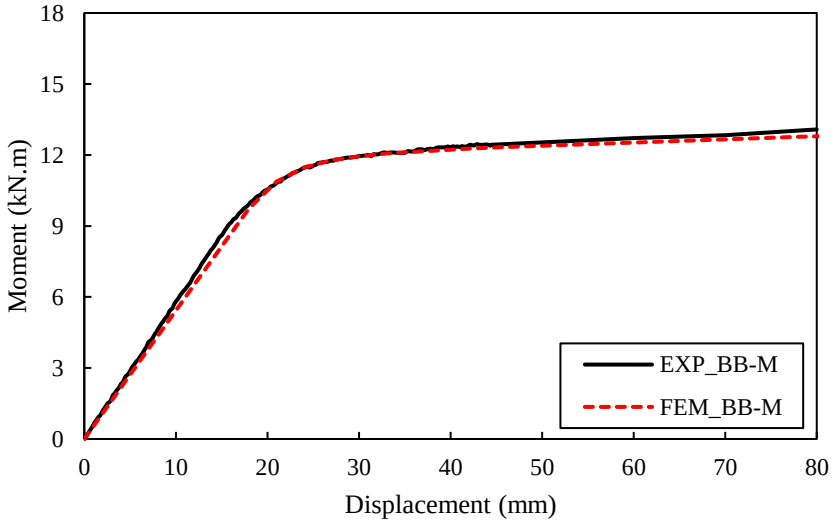

Figure 3: Experimental and FE model moment capacity vs displacement curves of the bare CHS members (BB-M)

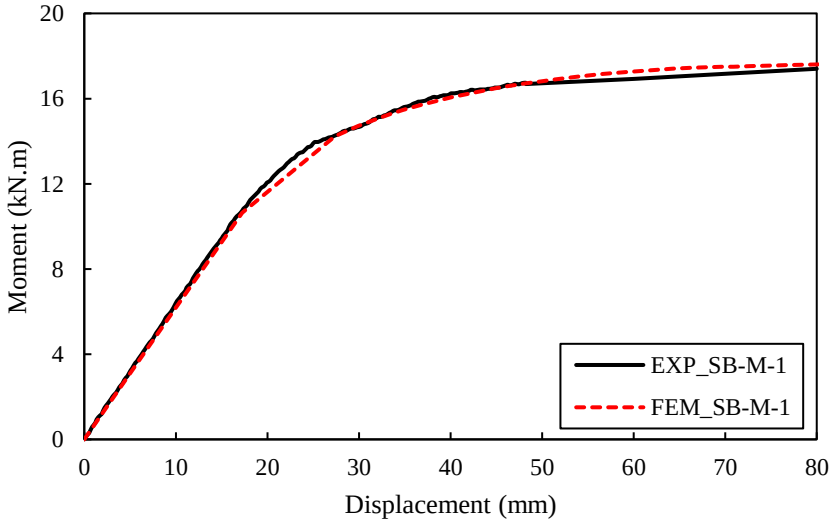

Figure 4: Experimental and FE model moment capacity curves of the CFRP strengthened steel member (SB-M-1)

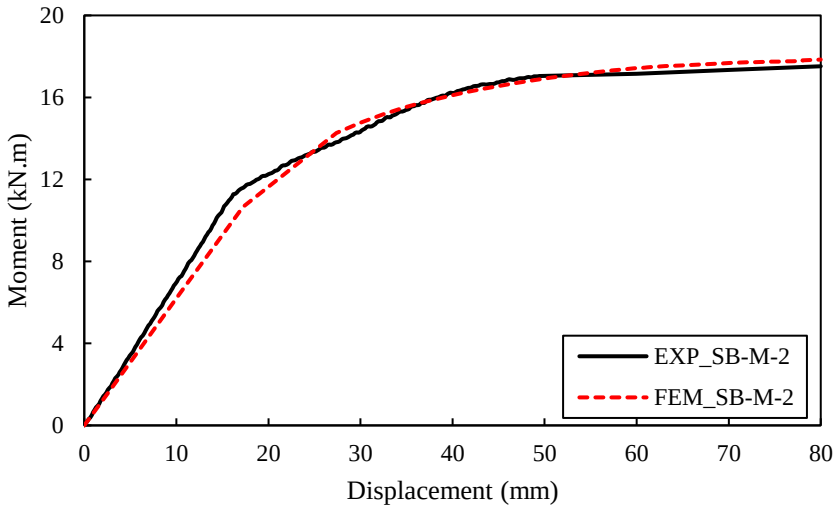

Figure 5: Experimental and FE model moment capacity curves of the CFRP strengthened steel member (SB-M-2)

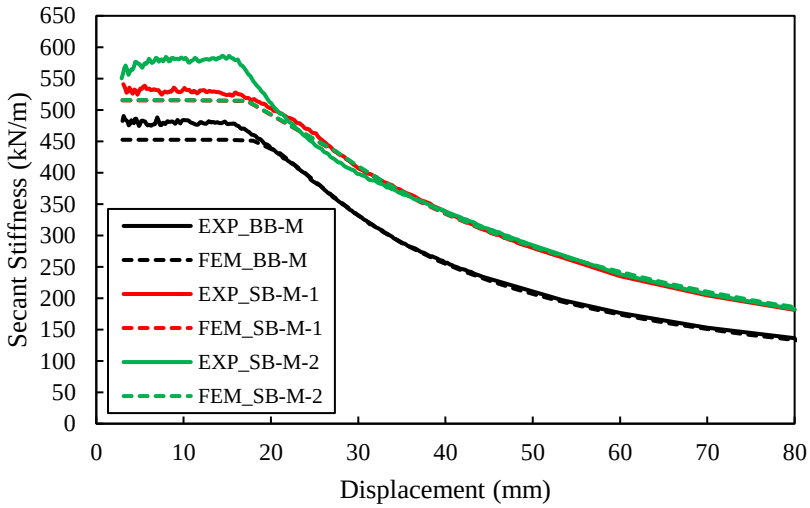

Figure 6: Experimental and FE model secant stiffness versus displacement curves of the bare (BB-M) and CFRP strengthened steel members (SB-M-1 and SB-M-2)

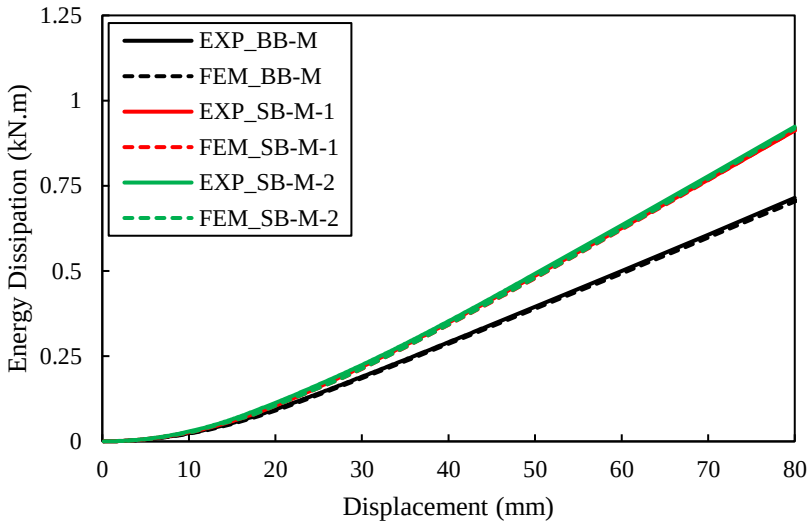

Figure 7: Experimental and FE model Energy dissipation capacities vs dsiplacement of the bare (BB-M) and CFRP strengthened steel members (SB-M-1 and SB-M-2)

4. Parametric Study on CFRP strengthened RHS

A detailed parametric study is conducted to investigate the effects of a range of parameters such as the bond length, number of CFRP layers, ratio of CFRP thickness to CHS wall thickness, diameter to thickness ratio of CHS and steel grade of CHS on the behaviour of CFRP strengthened CHS members under monotonic loading. Effects of bond length and number of layers of CFRP are considered in order to minimize the cost of the CFRP strengthening by finding structurally sound but cost effective bond length and number of layers of CFRP, as after certain bond length and number of layers of CFRP, there is very little or no change in the structural performance of CFRP strengthened steel members [18]. In addition, the effect of the ratio of CFRP thickness to CHS wall thickness and the diameter to thickness ratio of CHS were investigated as authors wanted to and were able to establish that the compactness of steel section has a significant effect on the performance of CFRP strengthened steel members [18]. Moreover, the effect of steel grade is considered to get more results in different steel grade as higher grades of steel are being used more frequently.

4.1 Effect of bond length of CFRP

The CFRP was applied with a bond length of 900 mm (which was 82% of the total specimen length) from the fixed end to strengthen the CHS specimens. To minimise the overall cost of civil engineering strengthening projects with CFRP, an investigation on effective bond length of CFRP composites is very important. To determine the most effective bond length of CFRP composites under monotonic load case for CHS members, the wrapping length of the CFRP was varied. CHS steel members were strengthened with four different CFRP bond lengths. In addition to the 900mm (as in the experimentally tested specimens) lengths of 200 mm, 300 mm and 400 mm bond lengths were considered. Only the Mbrace saturant was used in the FE models in all the parametric studies as the experimental study concluded that adhesives do not have much effect on the strengthening [16]. Structural responses in terms of moment capacity curves, maximum moment capacity, secant stiffness, energy dissipation capacity and ductility factor are compared in Figure 8, Figure 9, Figure 10, Figure 11 and Figure 12 respectively. The ductility factor is calculated by dividing the energy at the ultimate load by the elastic energy [26]. An improvement in the structural performance under monotonic loading can be seen from Figure 8–Figure 12 for the CFRP strengthened steel members as the bond length increases up to a 400 mm bond length. This improvement is seen in the higher maximum moment capacity, stiffness, energy dissipation capacity and ductility factor. However, CFRP bond lengths greater than 400 mm showed little or no change in structural performance for the strengthened CHS members. The ultimate moment capacity of strengthened CHS members using 100 mm, 200 mm, 300 mm, 400 mm, 600 mm, and 900 mm showed increase of 9.37%, 20.23%, 30.53%, 36.32%, 37.52 and 37.63% respectively over the bare steel CHS member. Hence, a bond length of 400 mm is the most effective which has been used in further parametric studies.

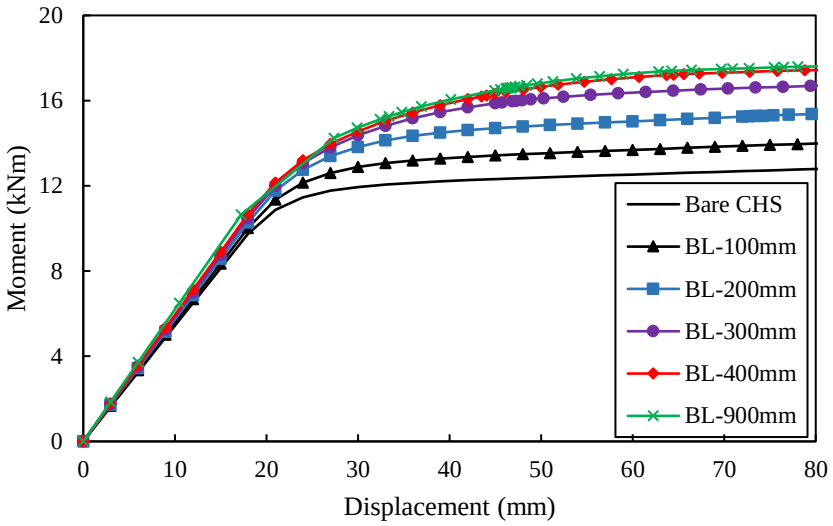

Figure 8: Moment capacity curves of CFRP strengthened CHS members with different bond lengths of CFRP

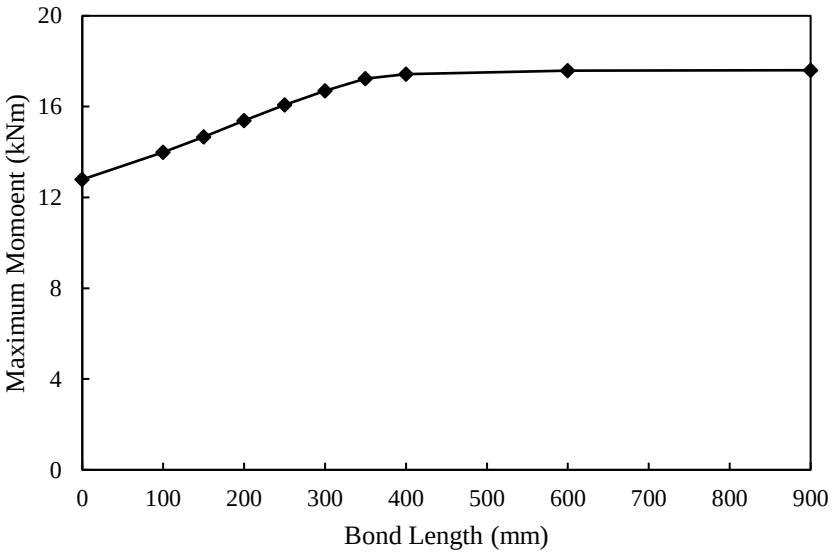

Figure 9: Maximum moment capacities of CFRP strengthened CHS members with different bond lengths of CFRP

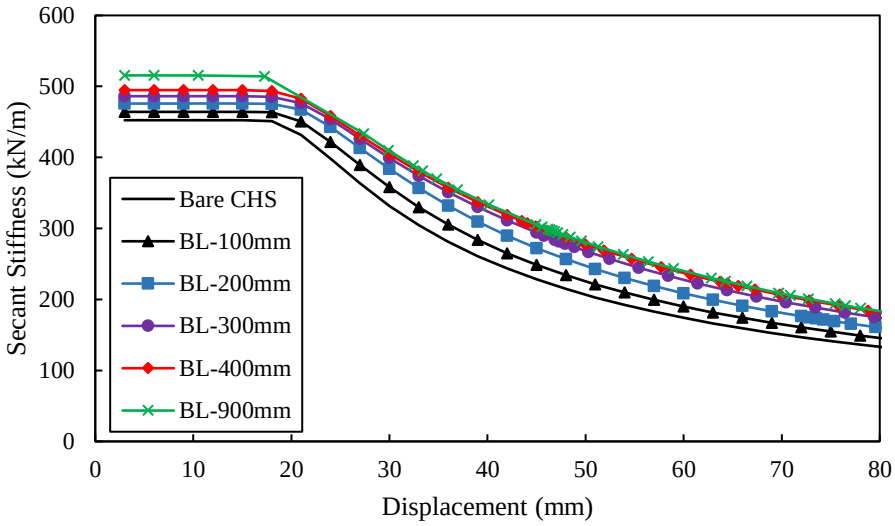

Figure 10: Secant stiffness curves of CFRP strengthened CHS members with different bond lengths of CFRP

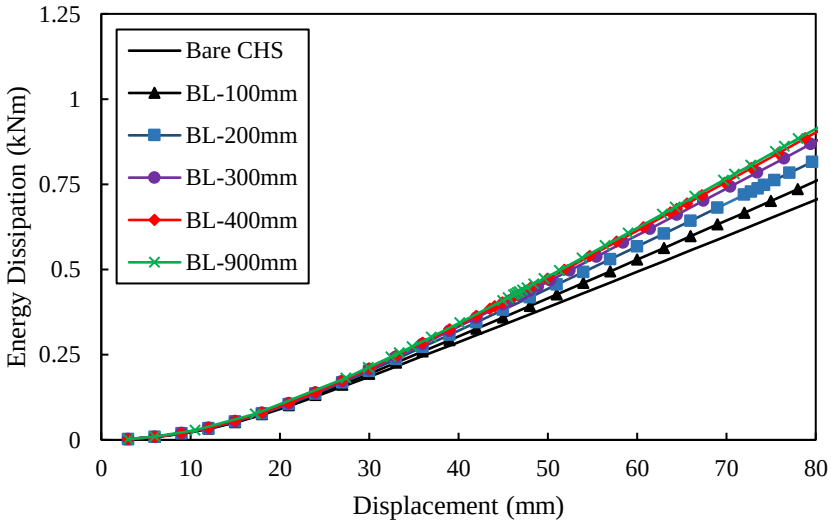

Figure 11: Energy dissipation capacities of CFRP strengthened CHS members with different bond lengths of CFRP

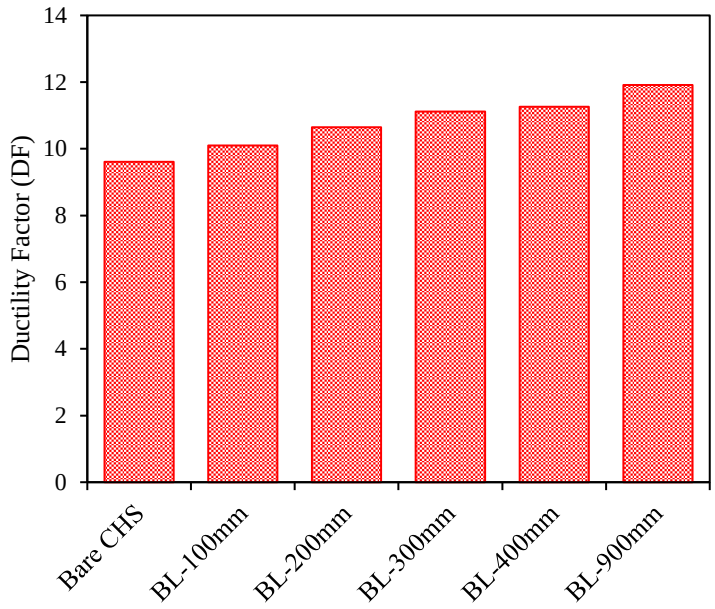

Figure 12: Ductility factor of CFRP strengthened CHS members with different bond lengths of CFRP

4.2 Effect of number of CFRP layers

To determine the most effective number of CFRP layers for strengthening the CHS steel members the bond length 400 mm was kept constant while CFRP composites of 1, 2, 3 and 4 layers were used to strengthen the members. The structural responses in terms of moment capacity curves, maximum moment capacity, secant stiffness, energy dissipation capacity and ductility factor are compared in Figure 13, Figure 14, Figure 15, Figure 16 and Figure 17 respectively. It can be seen from Figure 13-Figure 17 that all the structural response parameters improved up to strengthening with 3 layers of CFRP. The effect however, of increasing the number of CFRP composite layers past 3 layers is seen to have an insignificant effect on the different structural responses of the strengthened CHS steel members under monotonic loading. Hence, it can be concluded that with an increase in the number of CFRP composite layers to strengthen CHS steel members, the structural performance of the member is increased. Additionally, the most cost-effective and efficient number of CFRP composite layers to strengthen the CHS steel members is 3 layers. Civil engineering infrastructure projects can

minimise the costs by using this parametric study to find the required optimal layer numbers of CFRP.

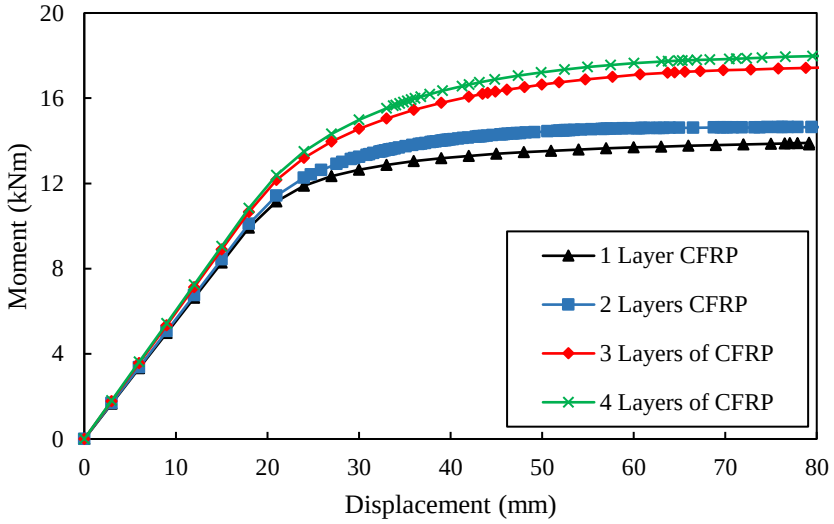

Figure 13: Moment capacity curves for CFRP strengthened CHS members with different number of layers of CFRP

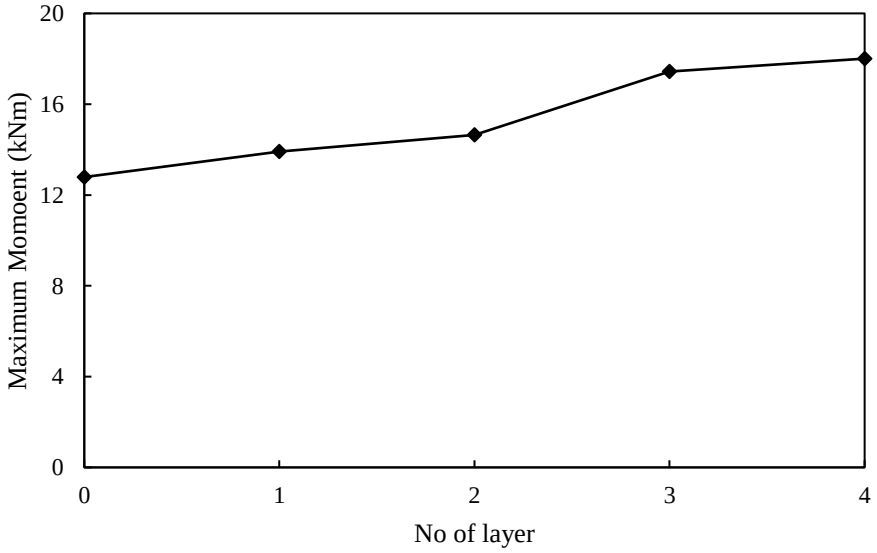

Figure 14: Maximum moment capacities of CFRP strengthened CHS members with different number of layers of CFRP

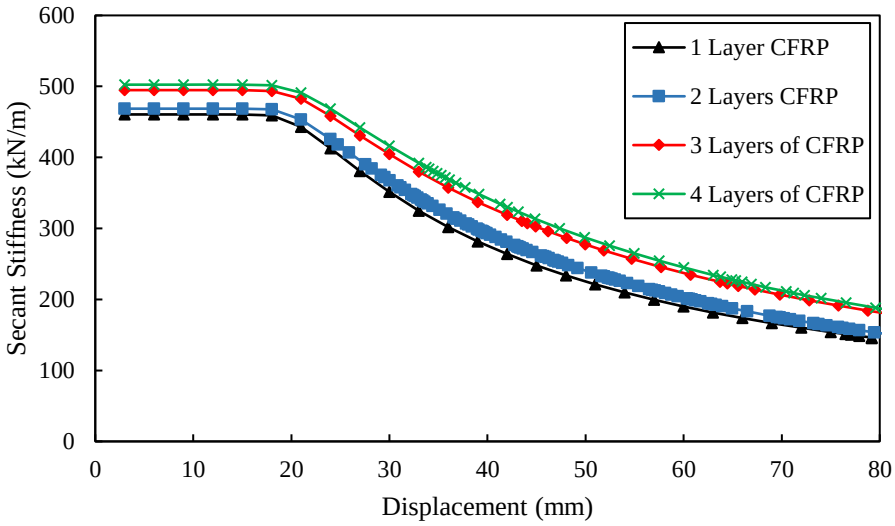

Figure 15: Secant stiffness curves for CFRP strengthened CHS members with different number of CFRP layers.

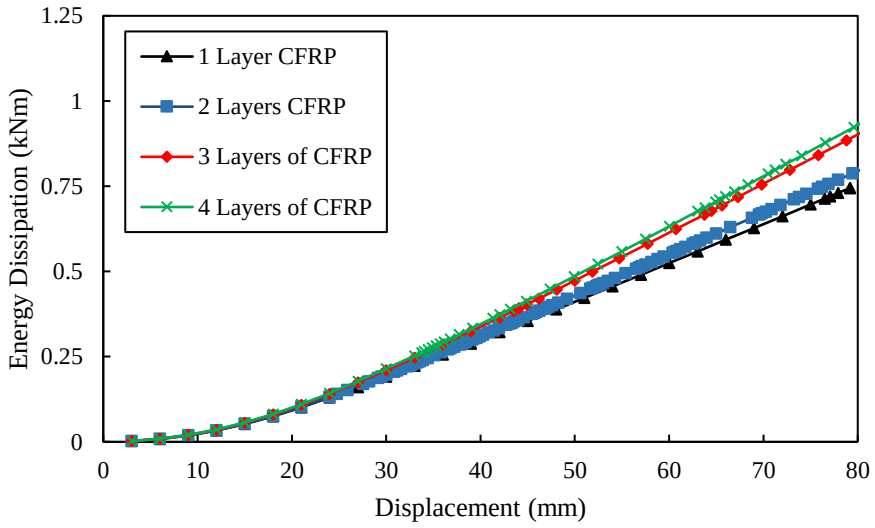

Figure 16: Energy dissipation capacities of CFRP strengthened CHS members with different number of layers of CFRP

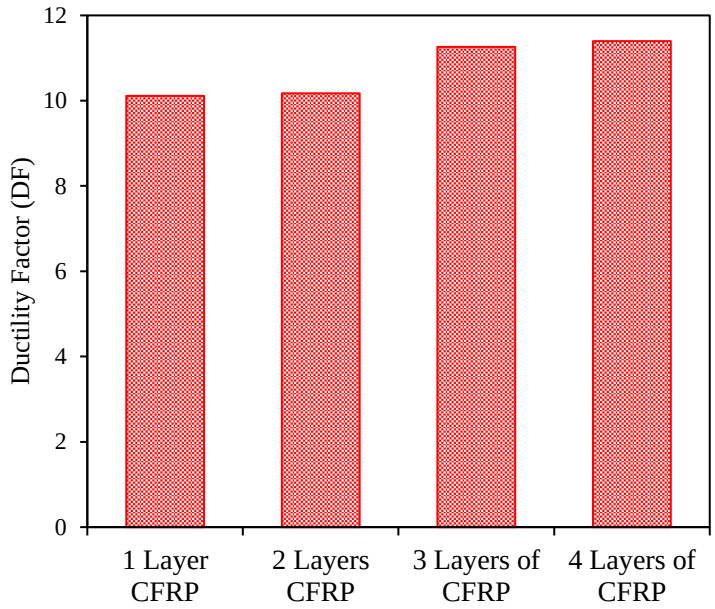

Figure 17: Ductility factor of CFRP strengthened CHS members with different number of layers of CFRP

4.3 Effect of t_{CFRP}/t_{CHS} ratio

Thus far, it has been shown that 3 layers of CFRP composite along with 400 mm bond length have shown to be most effective for strengthening CHS steel members under monotonic loading. Hence, 3 layers of CFRP composite along with a 400 mm bond length will be considered to determine the effects of the remaining parameters.

Three separate CHS steel members with 101.6 mm outside diameter but varying wall thicknesses from 3.2 mm, 3.6 mm and 4.0 mm are considered to investigate the effect of t_{CFRP}/t_{CHS} ratio on the structural performance of CHS steel members strengthened with CFRP under monotonic loading. The ratio of the CFRP thickness to CHS wall thickness decreases with the increase in wall thickness of the CHS from 3.2 mm to 3.6 mm to 4 mm as all the CHS specimens are strengthened with 3 layers of CFRP. All the CFRP strengthened CHS steel members showed an improvement in the moment capacity, secant stiffness, energy dissipation capacity and ductility compared to their bare counterparts. The moment capacity-displacement

curves for all the bare and CFRP strengthened CHS members are shown in Figure 18. CFRP strengthening enhanced the ultimate moment capacity of 101.6×3.2, 101.6×3.6, and 101.6×4.0 from 10.49 kNm to 14.95 kNm, 11.78 kNm to 16.34 kNm and 12.79 kNm to 17.45 kNm respectively. This shows an improvement of the maximum moment capacities by 42.5%, 38.69% and 36.46% over the bare CHS for the wall thickness of 3.2 mm, 3.6 mm and 4.0 mm respectively.

The comparisons of the secant stiffness–displacement curves of the bare and CFRP strengthened CHS specimens are shown in Figure 19. All the CFRP strengthened CHS members have shown a better performance over their bare counterparts in terms of secant stiffness under monotonic loading. The CFRP strengthened CHS with wall thicknesses of 3.2 mm, 3.6 mm and 4 mm were showed 11.21%, 10.18% and 9.36% higher secant stiffness respectively compared to their bare counterparts. Figure 20 shows the comparison of the energy dissipation capacities of the bare and CFRP strengthened CHS members with different wall thicknesses. At the initial displacement, both bare and CFRP strengthened CHS specimens exhibit almost the same energy dissipation due to their high initial stiffness. At the ultimate displacement, the energy dissipation of the CFRP strengthened CHS members with wall thicknesses of 3.2 mm, 3.6 mm and 4 mm show an enhancement of 32.84%, 29.85% and 28.11% respectively compared to their bare counterparts. The ductility factor of the bare and CFRP strengthened members have been compared in Figure 21 where all of the CFRP strengthened CHS specimens showed higher ductility over the bare CHS specimens.

Figure 22, Figure 23 and Figure 24 are display the comparison of the failure modes of the bare steel section and the CFRP strengthened section with wall thicknesses of 3.2 mm, 3.6 mm and 4 mm respectively. It can be noticed that the local buckling has been delayed and reduced due to the CFRP strengthening technique for all the CHS specimens. This is due to the contribution

of the strengthening CFRP composites which have increased the stiffness of CHS and distributed the stresses from the critical region to cover the whole section more uniformly.

This investigation shows that the ratio of the CFRP thickness to CHS wall thickness greatly influences the all the cited structural response parameters under monotonic loading. The effectiveness of this technique for strengthening CHS steel with CFRP is shown to increase with the increase of the ratio of the CFRP thickness to CHS wall thickness.

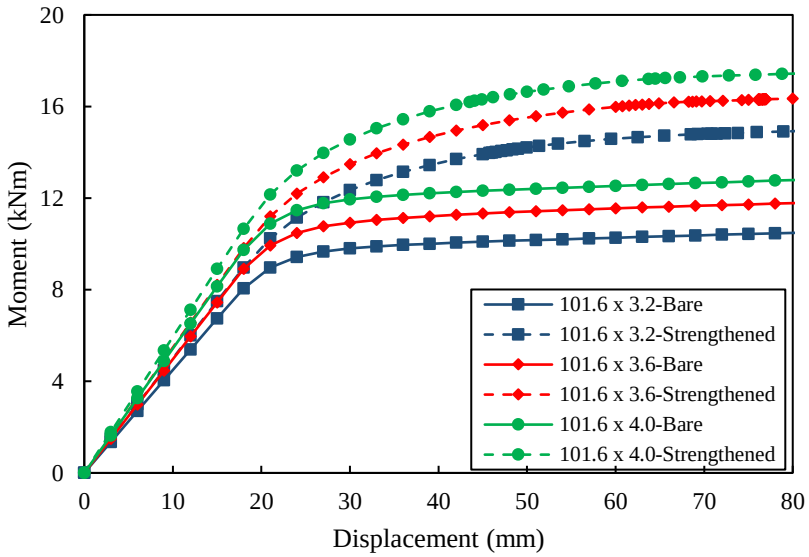

Figure 18: Moment capacities curves of bare and CFRP strengthened CHS members with different CFRP thickness to CHS wall thickness ratio

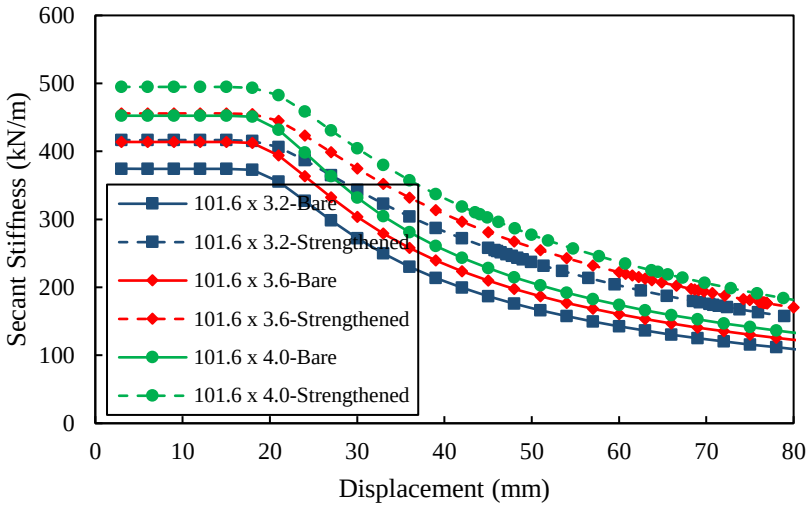

Figure 19: Secant stiffness curves for CFRP strengthened CHS members with different CFRP thickness to CHS wall thickness ratio

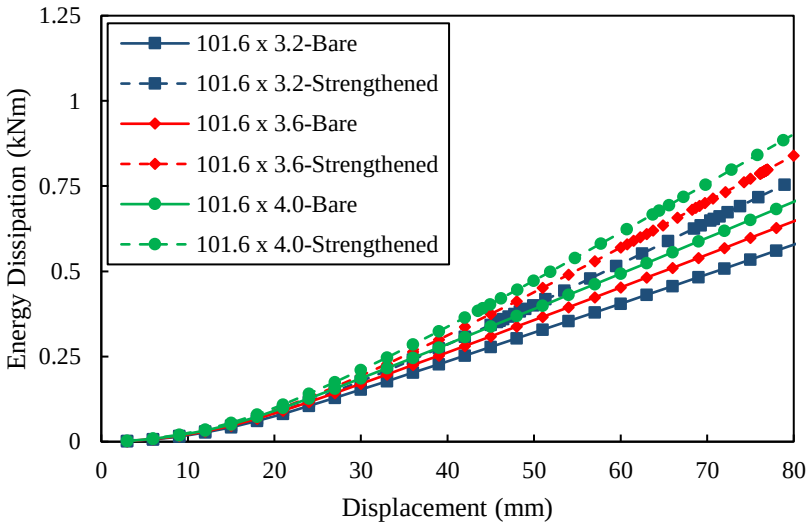

Figure 20: Energy dissipation capacities of CFRP strengthened CHS members with different CFRP thickness to CHS wall thickness ratio

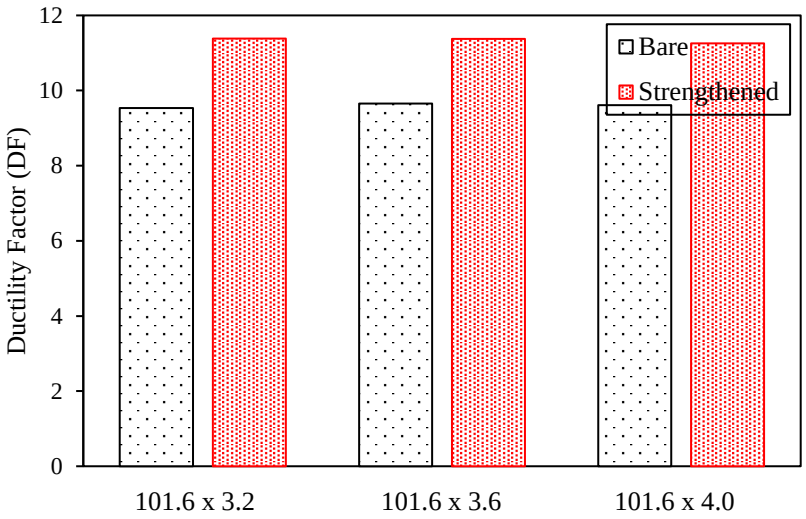

Figure 21: Ductility factor of CFRP strengthened CHS members with different CFRP thickness to CHS wall thickness ratio

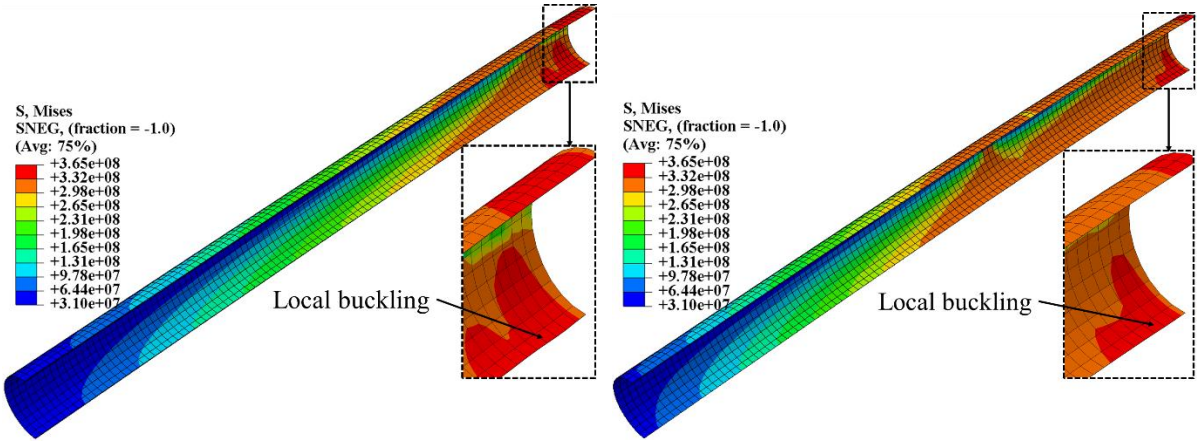

(a) (b)

Figure 22: Failure modes of steel section of (a) bare and (b) CFRP strengthened 101.6 ×3.2 CHS members

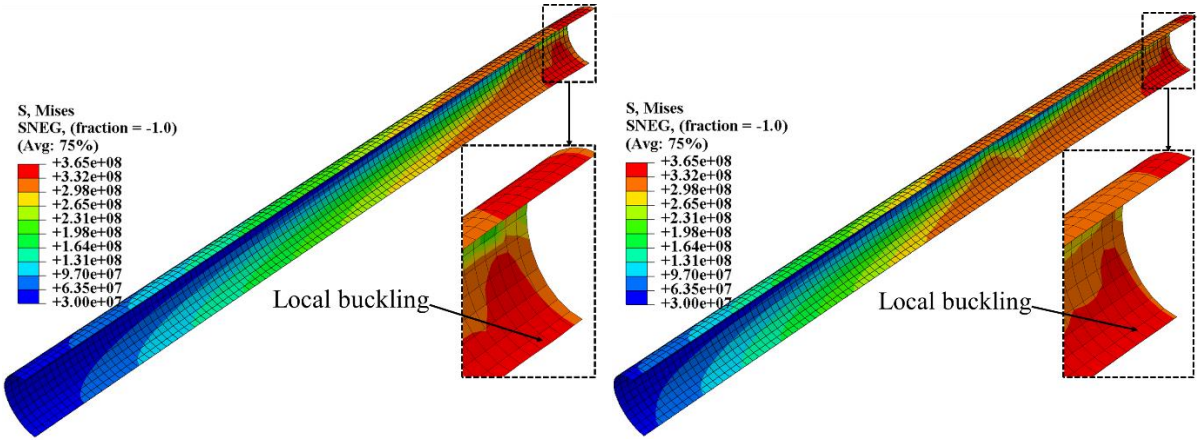

(a) (b)

Figure 23: Failure modes of steel section of (a) bare and (b) CFRP strengthened 101.6 ×3.6 CHS members

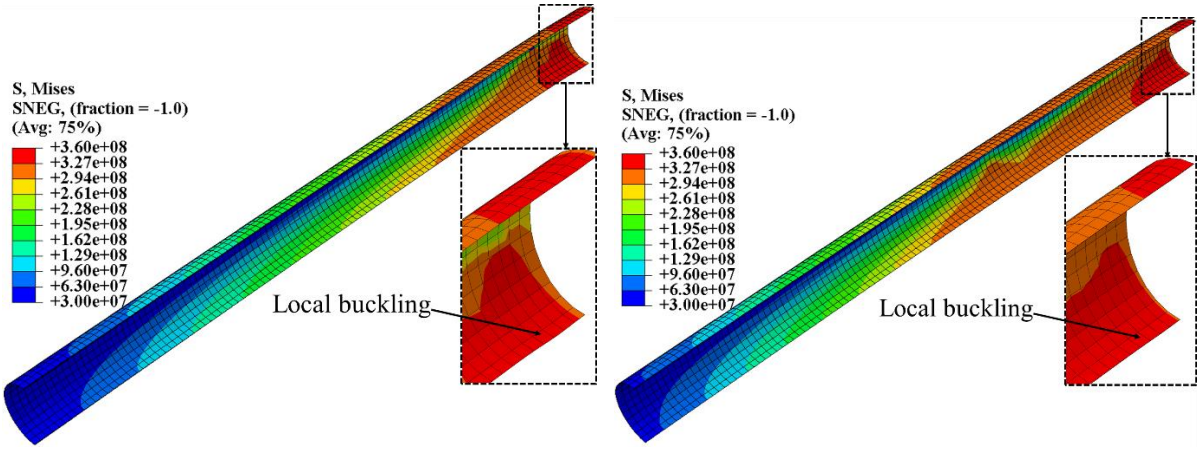

(a) (b)

Figure 24: Failure modes of steel section of (a) bare and (b) CFRP strengthened 101.6 ×4.0 CHS members

4.4 Effect of diameter to thickness ratio of CHS

The effect of the diameter to thickness ratio of CHS on the structural behaviour of bare and CFRP strengthened CHS specimens under monotonic loading are investigated by considering two new CHSs 139.7×4.0 and 193.7×4.0 along with the previous the CHSs 101.6×4.0. As the CHS wall thickness (4 mm) was kept constant, the diameter to thickness ratio of CHS increases with increase in its outer diameter. Figure 25-Figure 28 demonstrate that although all of the

CFRP strengthened CHS steel members showed an improvement in the moment capacity, secant stiffness, energy dissipation capacity and ductility compared to their bare counterparts, the increments in these performance factors were different. The CFRP strengthened CHS member with outer diameters of 101.6 mm, 139.7 mm and 193.7 mm showed increments in the ultimate maximum moment capacity by 36.46%, 39.83% and 45.96% respectively compared to their bare counterparts. It has been concluded in a previous study under four-point bending test [13] that CFRP strengthening technique becomes increasingly effective when the compactness of the CHS specimens decrease. Hence, the effectiveness of the CFRP strengthening technique is enhanced with the increase in the diameter to thickness ratio of CHS. A similar feature was also evident when the thickness of the CHS section was decreased as shown in the previous section. This is so as both increase in the diameter to thickness ratio and reduction in wall thickness of the CHS members cause a reduction in the compactness of the CHS member. Thus, it can be concluded that increment predictions of the various structural performance factors due to CFRP strengthening of a particular CHS specimen under monotonic loading cannot be utilised for other CHS steel members with different diameter to thickness ratios or different wall thicknesses, even if all the other parameters remain constant. The FE model developed in the present study will be highly effective to predict the increments of structural performance factors by CFRP strengthening technique under monotonic load cases for various CHS steel members whose material and geometric properties are known.

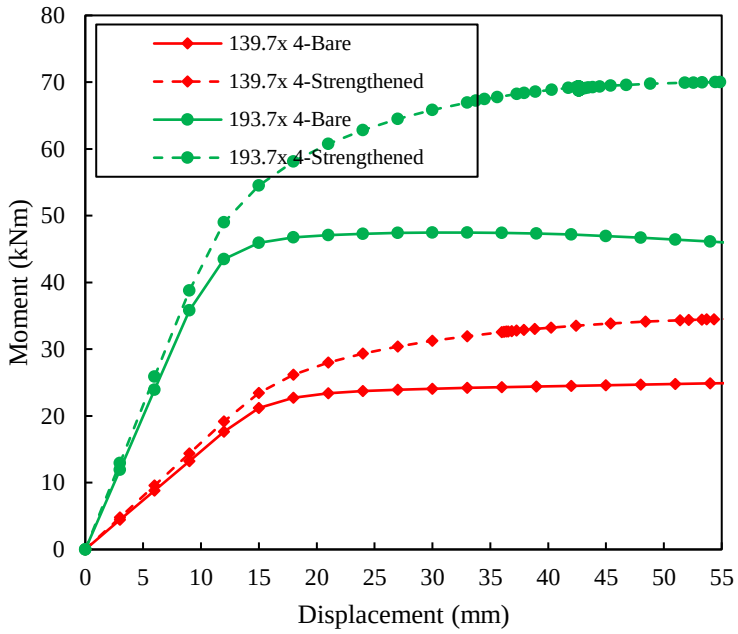

Figure 25: Moment capacities curves of bare and CFRP strengthened CHS members with different diameter to thickness ratio

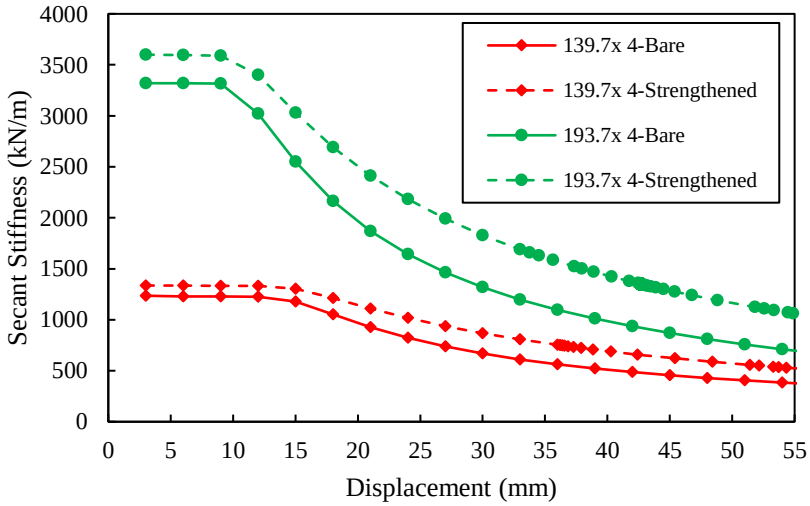

Figure 26: Secant stiffness curves for CFRP strengthened CHS members with different diameter to thickness ratio

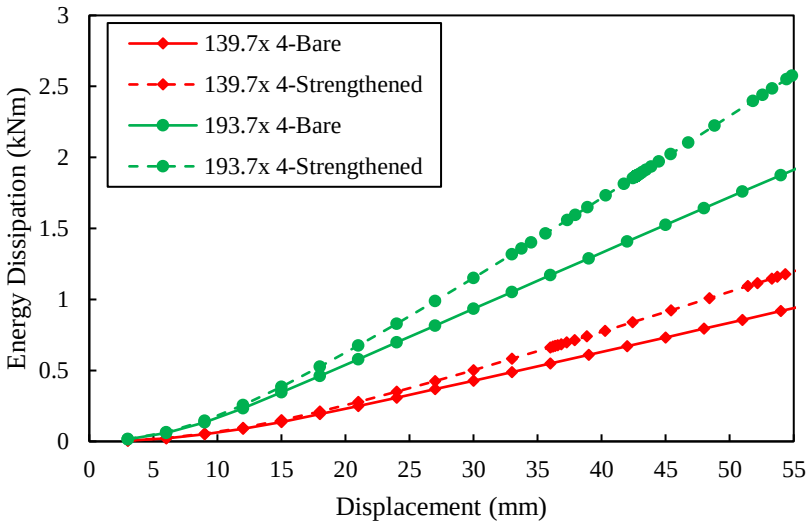

Figure 27: Energy dissipation capacities of CFRP strengthened CHS members with different diameter to thickness ratio

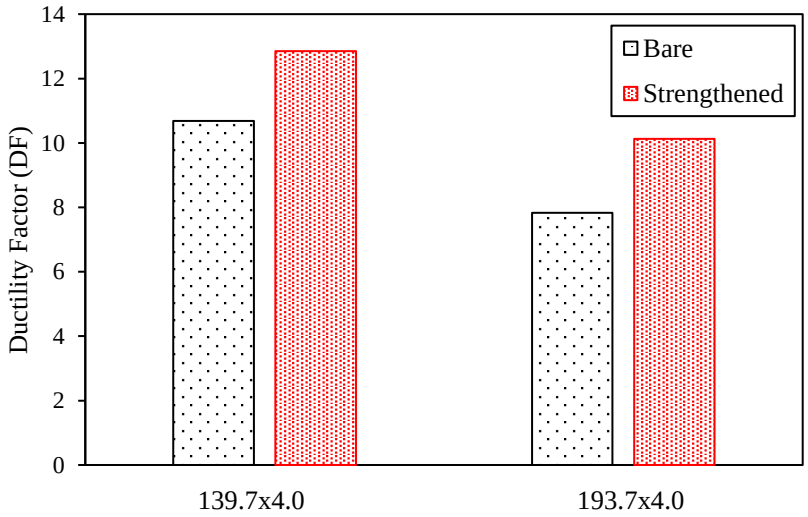

Figure 28: Ductility factor of CFRP strengthened CHS members with different diameter to thickness ratio

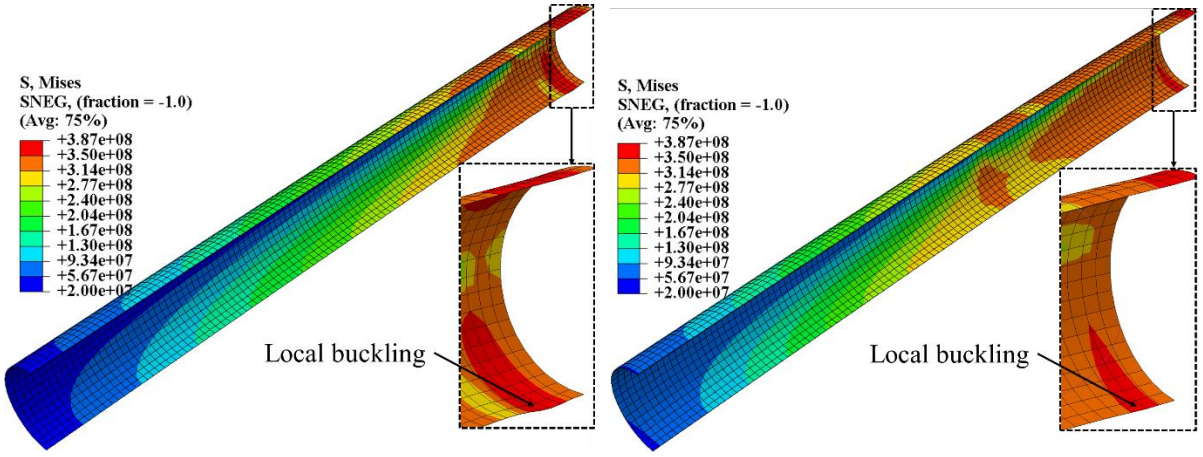

(a) (b)

Figure 29: Failure modes of steel section of (a) bare and (b) CFRP strengthened 139.7×4.0 CHS members

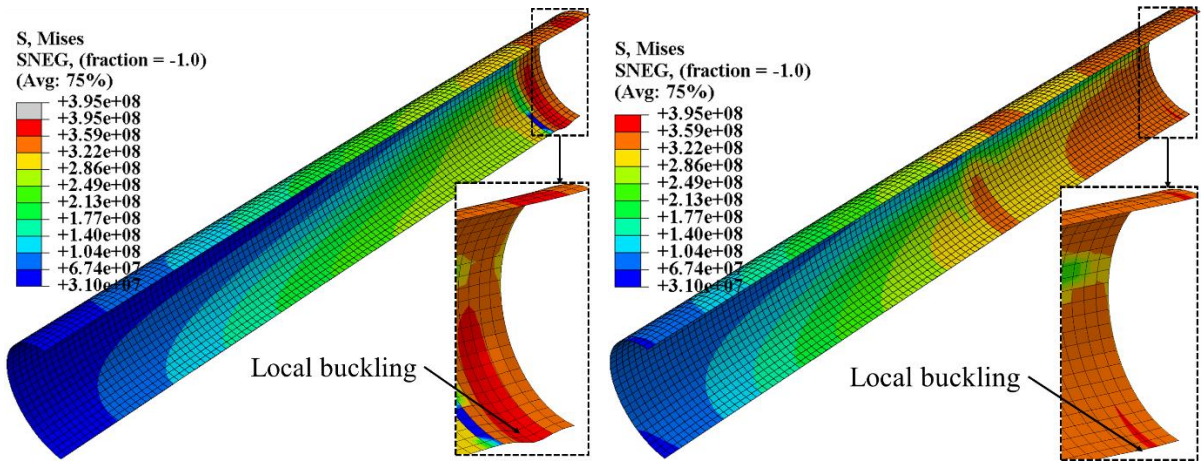

(a) (b)

Figure 30: Failure modes of steel section of (a) bare and (b) CFRP strengthened 193.7×4.0 CHS members

4.5 Effect of steel grade

Steel grade is an extremely important parameter for steel members, especially as higher grades of steel are being used more frequently. Three different steel grades of 250 GPa, 350 GPa and 450 GPa were selected while the CHS 101.6×4 mm was selected (as a constant) for investigating the effect of steel grade on the structural performance of the CFRP strengthened CHS under monotonic load. The performance parameters with respect to moment capacity

curves, secant stiffness, energy dissipation and ductility of the bare and strengthened specimens with different steel grades are compared in Figure 31, Figure 32, Figure 33 and Figure 34. The effectiveness of the CFRP strengthening method for each steel grade can be seen in these figures and it is evident that the effectiveness reduces with increase of the steel grade.

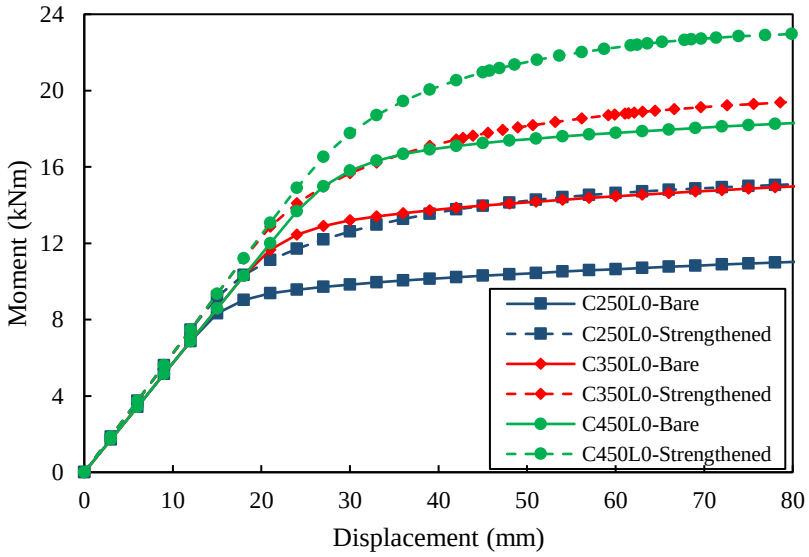

Figure 31: Moment capacities curves of bare and CFRP strengthened CHS members with different steel-grades

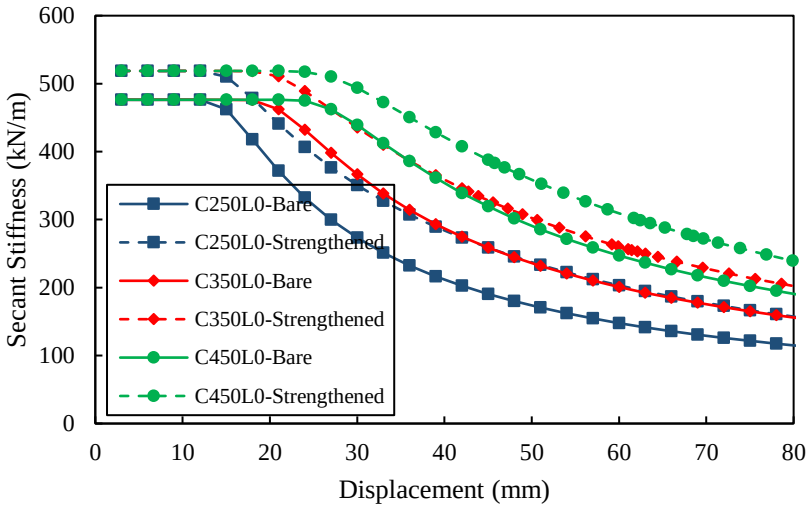

Figure 32: Secant stiffness curves for CFRP strengthened CHS members with different steel-grades

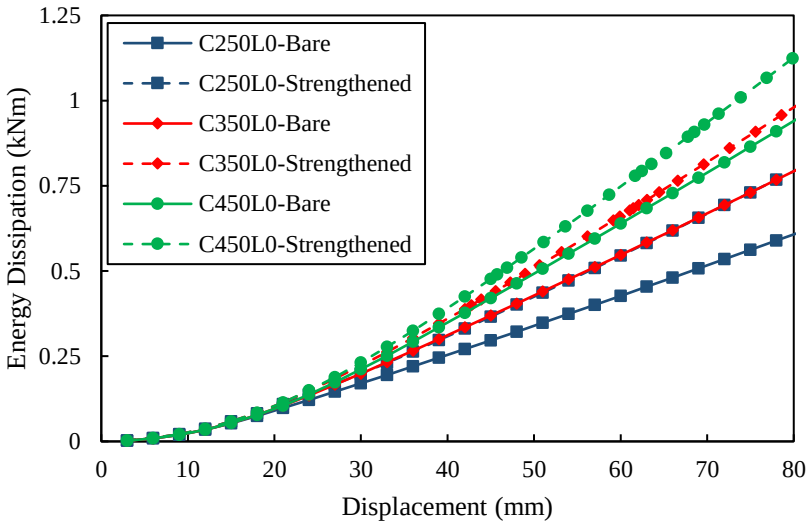

Figure 33: Energy dissipation capacities of CFRP strengthened CHS members with different steel-grades

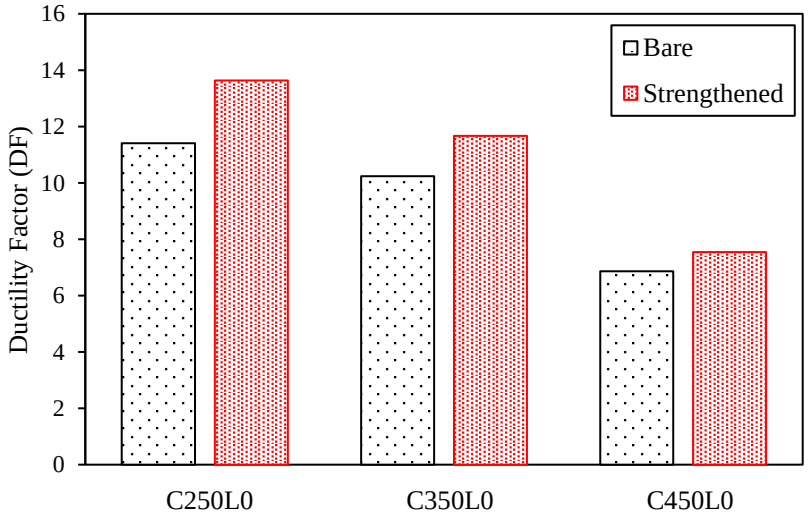

Figure 34: Ductility factor of CFRP strengthened CHS members with different steel-grades

5. Conclusions

A detailed numerical study has been carried out to evaluate the structural response of CFRP strengthened CHSs under monotonic loading. The FE model used in this study was validated by comparing the FE simulated results with the authors' published experimental results. Additionally, a parametric study was performed to determine the effects of CFRP bond length,

number of CFRP layers, ratio of CFRP thickness to CHS wall thickness, diameter to thickness ratio of CHS and steel grade on the structural response of the strengthened CHS specimens in terms of moment capacity, secant stiffness, energy dissipation and ductility. Based on the results of the present investigation the following conclusions can be drawn:

i. The developed FE model can effectively predict the structural responses of bare and CFRP strengthened steel CHS members with various CFRP thickness to CHS wall thickness ratios, diameter to thickness ratios and steel grades under monotonic loading. This information is important and can be obtained through numerical simulations using the proposed FE model with great savings in cost and time compared to experimental investigations.

ii. CFRP strengthened CHS steel members using a bond length of 400 mm and CFRP composite layers of 3 are the most cost-effective option for increasing the different structural performance indicators under monotonic loading. There is very little or no effect on these indicators when the bond length or number of CFRP layers are increased beyond.

iii. The effectiveness of the CFRP strengthening increases with an increase in the ratio of CFRP composite thickness to CHS wall thickness.

iv. The effectiveness of CFRP strengthening increases with an increase in the CHS diameter to wall thickness ratio as this results in a reduction in the compactness of the section.

v. The effectiveness of the CFRP strengthening technique has been confirmed for all steel grades although the effectiveness is reduced with an increase in the steel grade.

Acknowledgment

The authors would like to thank Queensland University of Technology (QUT) for providing support (the high-performance computer (HPC) facility, software for analysis) to carry out the work reported in this paper.

Data Availability Statement

The raw/processed data required to reproduce these findings cannot be shared at this time as the data also forms part of an ongoing study.

References

[1] J. Wardenier, J.A. Packer, X.L. Zhao, G.J. Van der Vegte, Hollow sections in structural applications, Bouwen met Staal Rotterdam,, The Netherlands, 2002.

[2] M. V. Seica, J.A. Packer, FRP materials for the rehabilitation of tubular steel structures, for underwater applications, Compos. Struct. 80 (2007) 440–450. doi:10.1016/j.compstruct.2006.05.029.

[3] Tafsirojjaman, S. Fawzia, D. Thambiratnam, Enhancement Of Seismic Performance Of Steel Frame Through CFRP Strengthening, Procedia Manuf. 30 (2019) 239–246. doi:10.1016/j.promfg.2019.02.035.

[4] C. Batuwitage, S. Fawzia, D.P. Thambiratnam, T. Tafsirojjaman, R. Al-Mahaidi, M. Elchalakani, CFRP-wrapped hollow steel tubes under axial impact loading, in: Tubul. Struct. XVI Proc. 16th Int. Symp. Tubul. Struct. (ISTS 2017, 4-6 December 2017, Melbourne, Aust., CRC Press, 2017: p. 401.

[5] X.L. Zhao, L. Zhang, State-of-the-art review on FRP strengthened steel structures, Eng. Struct. 29 (2007) 1808–1823. doi:10.1016/j.engstruct.2006.10.006.

[6] T. Tafsirojjaman, S. Fawzia, D. Thambiratnam, Numerical investigation on the CFRP

strengthened steel frame under earthquake, in: Mater. Sci. Forum Front. Compos. Mater. IV, Trans Tech Publications Ltd., 2019.

[7] M.I. Alam, S. Fawzia, T. Tafsirojjaman, X.L. Zhao, FE modeling of FRP strengthened CHS members subjected to lateral impact, in: Tubul. Struct. XVI Proc. 16th Int. Symp. Tubul. Struct. (ISTS 2017, 4-6 December 2017, Melbourne, Aust., CRC Press, 2017: p. 409.

[8] T. Tafsirojjaman, S. Fawzia, D. Thambiratnam, X.L. Zhao, Seismic strengthening of rigid steel frame with CFRP, Arch. Civ. Mech. Eng. 19 (2019) 334–347. doi:10.1016/j.acme.2018.08.007.

[9] T. Tafsirojjaman, S. Fawzia, D. Thambiratnam, Numerical investigation on the seismic strengthening of steel frame by using normal and high modulus CFRP, in: Proc. Seventh Asia-Pacific Conf. FRP Struct., International Institute for FRP in Construction (IIFC), 2019.

[10] N.D. Fernando, Bond behaviour and debonding failures in CFRP-strengthened steel members, The Hong Kong Polytechnic University, 2010.

[11] K.A. Harries, A.J. Peck, E.J. Abraham, Enhancing stability of structural steel sections using FRP, Thin-Walled Struct. 47 (2009) 1092–1101. doi:10.1016/j.tws.2008.10.007.

[12] M.H. Kabir, S. Fawzia, T.H.T. Chan, J.C.P.H. Gamage, J.B. Bai, Experimental and numerical investigation of the behaviour of CFRP strengthened CHS beams subjected to bending, Eng. Struct. 113 (2016) 160–173. doi:10.1016/j.engstruct.2016.01.047.

[13] J. Haedir, M.R. Bambach, X.L. Zhao, R.H. Grzebieta, Strength of circular hollow sections (CHS) tubular beams externally reinforced by carbon FRP sheets in pure bending, Thin-Walled Struct. 47 (2009) 1136–1147. doi:10.1016/j.tws.2008.10.017.

[14] M.H. Kabir, S. Fawzia, T.H.T. Chan, M. Badawi, Durability of CFRP strengthened steel circular hollow section member exposed to sea water, Constr. Build. Mater. 118 (2016) 216–225. doi:10.1016/j.conbuildmat.2016.04.087.

[15] M.H. Kabir, S. Fawzia, T.H.T. Chan, Durability of CFRP strengthened circular hollow steel members under cold weather: Experimental and numerical investigation, Constr. Build. Mater. 123 (2016) 372–383. doi:10.1016/j.conbuildmat.2016.06.116.

[16] T. Tafsirojjaman, S. Fawzia, D. Thambiratnam, X.L. Zhao, Behaviour of CFRP strengthened CHS members under monotonic and cyclic loading, Compos. Struct. 220 (2019) 592–601. doi:10.1016/j.compstruct.2019.04.029.

[17] SIMULIA, ABAQUS 6.19, ABAQUS Anal. Theory Manuals, SIMULIA, Dassault Systèmes, Realis. Simulation, Provid. RI, USA. (2019).

[18] T. Tafsirojjaman, S. Fawzia, D. Thambiratnam, X. Zhao, Numerical investigation of CFRP strengthened RHS members under cyclic loading, Structures. 24 (2020) 610–626. doi:10.1016/j.istruc.2020.01.041.

[19] J.G. Teng, D. Fernando, T. Yu, Finite element modelling of debonding failures in steel beams flexurally strengthened with CFRP laminates, Eng. Struct. 86 (2015) 213–224. doi:10.1016/j.engstruct.2015.01.003.

[20] A. Al-Mosawe, R. Al-Mahaidi, X.L. Zhao, Effect of CFRP properties, on the bond characteristics between steel and CFRP laminate under quasi-static loading, Constr. Build. Mater. 98 (2015) 489–501. doi:10.1016/j.conbuildmat.2015.08.130.

[21] M. Fadden, J. McCormick, Finite element model of the cyclic bending behavior of hollow structural sections, J. Constr. Steel Res. 94 (2014) 64–75. doi:10.1016/j.jcsr.2013.10.021.

[22] M.L. Benzeggagh, M. Kenane, Measurement of mixed-mode delamination fracture toughness of unidirectional glass/epoxy composites with mixed-mode bending apparatus, Compos. Sci. Technol. 56 (1996) 439–449.

[23] Z. Hashin, Failure criteria for unidirectional fibre composites, ASME J. Appl. Mech. 47 (1980) 329–334.

[24] Z. Hashin, A. Rotem, A fatigue failure criterion for fiber reinforced materials, J. Compos. Mater. 7 (1973) 448–464.

[25] F. Nunes, J.R. Correia, N. Silvestre, Structural behavior of hybrid FRP pultruded beams: Experimental, numerical and analytical studies, Thin-Walled Struct. 106 (2016) 201–217. doi:10.1016/j.tws.2016.05.004.

[26] A.P.C. Duarte, B.A. Silva, N. Silvestre, J. de Brito, E. Júlio, J.M. Castro, Tests and design of short steel tubes filled with rubberised concrete, Eng. Struct. 112 (2016) 274–286. doi:10.1016/j.engstruct.2016.01.018.